ARTIFICIAL MUSCLES

Unipolar stroke, electroosmotic pump carbon nanotube yarn muscles

Hetao Chu[1,2]*, Xinghao Hu[1,3]*, Zhong Wang[1,4]*, Jiuke Mu[1]*, Na Li[1,5], Xiaoshuang Zhou[6], Shaoli Fang[1], Carter S. Haines[1,7], Jong Woo Park[8], Si Qin[9], Ningyi Yuan[6], Jiang Xu[3], Sameh Tawfick[10], Hyungjun Kim[11,12], Patrick Conlin[11], Maenghyo Cho[11,12], Kyeongjae Cho[11], Jiyoung Oh[1], Steven Nielsen[4], Kevin A. Alberto[4], Joselito M. Razal[9], Javad Foroughi[13], Geoffrey M. Spinks[14], Seon Jeong Kim[8], Jianning Ding[3,6]†, Jinsong Leng[2]†, Ray H. Baughman[1]†

Success in making artificial muscles that are faster and more powerful and that provide larger strokes would expand their applications. Electrochemical carbon nanotube yarn muscles are of special interest because of their relatively high energy conversion efficiencies. However, they are bipolar, meaning that they do not monotonically expand or contract over the available potential range. This limits muscle stroke and work capacity. Here, we describe unipolar stroke carbon nanotube yarn muscles in which muscle stroke changes between extreme potentials are additive and muscle stroke substantially increases with increasing potential scan rate. The normal decrease in stroke with increasing scan rate is overwhelmed by a notable increase in effective ion size. Enhanced muscle strokes, contractile work-per-cycle, contractile power densities, and energy conversion efficiencies are obtained for unipolar muscles.

With the growing need for artificial muscles for diverse applications (*1*–*3*), major increases in muscle stroke, cycle rate, work capacity, power density, and energy conversion efficiency are required. Electrochemically driven muscles are especially important because their efficiencies are not restricted by the Carnot limit of thermal muscles and they can have a natural latching state, meaning that they can maintain stroke with low input energy.

The initially investigated electrochemical carbon nanotube (CNT) artificial muscles had a small stroke (~0.2%) (*4*, *5*), like that for many piezoelectrics, and their actuation was slow. Transitioning to twisted yarn electrochemical CNT muscles increased muscle stroke to 0.8% (*6*), and using coiled CNT yarns increased the contractile stroke for an organic electrolyte to up to 16.5% (*7*–*9*). Although muscle stroke can be amplified by mandrel coiling to make a muscle with a high spring index (the ratio of average coil diameter to yarn diameter) (*10*), this reduces the muscle's work capacity by disproportionally reducing load-lifting capability.

We provide solutions to a major problem for present electrochemical CNT yarn muscles. During a scan from extreme negative to extreme positive potentials, there is first an efflux of positive ions and then an influx of negative ions for the electrochemical double layer. Therefore, these muscles are bipolar, meaning that they first expand and then contract during this potential scan so that the net effect is a reduced overall stroke. By contrast, the stroke of a unipolar artificial muscle monotonically changes during a potential scan over the entire electrochemical window. Some of these unipolar muscles provide the strange property of increasing stroke with increasing potential scan rate, which we call scan rate–enhanced stroke (SRES).

Unlike bipolar electrochemical actuation, tensile actuation monotonically increases with temperature increases for thermally powered muscles (*11*–*13*) or weight increases for sorption-powered muscles (*14*). Unipolar tensile actuation is observed for Faradaic electrochemical muscles in which only one sign ion participates in an intercalation-based process over the available potential range (*15*, *16*). However, Faradaic intercalation generally suffers from rate and cyclability limitations, as seen by comparing battery and supercapacitor performance (*17*).

The artificial muscles were fabricated by inserting twist into a stack of forest-drawn or guest-containing CNT sheets (figs. S1 to S4) (*18*). The reported work capacities and power densities are for muscle contraction. For an optimized step potential change, the full-cycle power density is the ratio of contractile work-per-cycle to the cycle time, and the maximum average power density is the ratio of contractile work to actuation time for an optimized time (*19*). Unless otherwise noted, tensile actuation was characterized under constant load while the yarn was torsionally tethered, a large capacitance counter electrode was used, current densities are relative to the weight of dry muscle, and capacitances and injected charges are relative to the weight of CNTs. The performance metrics for bipolar muscles include only potential ranges where stroke cancellation does not occur.

The first investigated polymer guest was poly(sodium 4-styrenesulfonate) (PSS), which is approved for drug use and inexpensive enough for use in water softening. A CNT yarn containing PSS guest is called a PSS@CNT yarn. The dependence of measured strokes on the applied potential is shown in Fig. 1, A and B, for a bipolar neat CNT yarn and a unipolar PSS@CNT yarn, respectively, in 0.1 M aqueous LiCl electrolyte. About 30 weight percent (wt %) PSS was used to optimize performance. Piezoelectrochemical spectroscopy (PECS) indicates the origin of this transition from bipolar to unipolar actuation. During PECS, a cyclic voltammetry (CV) scan is conducted while the yarn is sinusoidally stretched (*20*). The potential of zero charge (pzc) is the potential at which the stretch-induced current change becomes zero (Fig. 1, C and D). PECS shows (figs. S5 and S6) that the pzc shift monotonically increases with increasing PSS concentration and converts to fully unipolar behavior for >5 wt % PSS because of a polymer-induced shift of the pzc from −80 mV to more than +1 V (which is outside the electrolyte's electrochemical stability window).

Although previous electrochemical yarn muscles decreased stroke with increasing potential scan rate (Fig. 1A), the stroke of this unipolar muscle containing 30 wt % PSS (Figs. 1B and 2A) increased (by a factor of 3.8 for a scan rate increase from 0.01 to 1 V/s, which is called the SRES enhancement). To evaluate the effects of scan rate on effective ion size (Fig. 2B), we measured the scan rate dependence of the stroke-charge ratio (SCR), the ratio of muscle stroke to the change in charge per CNT weight for a given potential scan range. These results show that the SCR of the neat

[1]Alan G. MacDiarmid NanoTech Institute, University of Texas at Dallas, Richardson, TX 75080, USA. [2]Center for Composite Materials and Structures, Harbin Institute of Technology (HIT), Harbin 150080, China. [3]Institute of Intelligent Flexible Mechatronics, Jiangsu University, Zhenjiang 212013, China. [4]Department of Chemistry and Biochemistry, University of Texas at Dallas, Richardson, TX 75080, USA. [5]MilliporeSigma, Materials Science, Milwaukee, WI 53209, USA. [6]Jiangsu Collaborative Innovation Center of Photovoltaic Science and Engineering, Changzhou University, Changzhou 213164, China. [7]Opus 12 Incorporated, Berkeley, CA 94710, USA. [8]Center for Self-Powered Actuation, Department of Biomedical Engineering, Hanyang University, Seoul 04763, South Korea. [9]Institute for Frontier Materials, Deakin University, Waurn Ponds, Victoria 3216, Australia. [10]Department of Mechanical Science and Engineering, University of Illinois Urbana-Champaign, Urbana, IL 61801, USA. [11]Department of Materials Science and Engineering, University of Texas at Dallas, Richardson, TX 75080, USA. [12]Department of Mechanical and Aerospace Engineering, Seoul National University, Gwanak-gu, Seoul 08826, The Republic of Korea. [13]Faculty of Engineering and Information Sciences, University of Wollongong, Australia, Wollongong, New South Wales 2500, Australia. [14]Intelligent Polymer Research Institute, Australian Institute for Innovative Materials, University of Wollongong, Wollongong, New South Wales 2522, Australia.
*These authors contributed equally to this work.
†Corresponding author. Email: dingjn@ujs.edu.cn (J.D.); lengjs@hit.edu.cn (J.L.); ray.baughman@utdallas.edu (R.H.B.)

CNT yarn is very low for both electron and hole injection and even slightly decreases in magnitude with increasing potential scan rate. However, the SCR for the PSS@CNT yarns generally increases with increasing scan rate (Fig. 2B). This result shows that the effective ion size increases with increasing potential scan rate because of the electroosmotic pumping of solvent. This effective ion size includes the ion hydration observed at low scan rates as well as the water dragged by the hydrated ion at high scan rates. Figure S17 shows that the coulombic efficiency is sufficiently high that charge loss minimally affects the SCR.

These results are like those known for electrochemically pumping water between ionomer membrane–separated reservoirs (*21*, *22*). Analogous water pumping has been observed for ionic polymer-metal composite (IPMC) bending actuators (*23*). Upon increasing the charge transfer rate, the hydrated ion drags additional water. If no ion solvation can occur, then SRES cannot result. This is demonstrated by the absence of SRES for actuation of PSS@CNT in an ionic liquid (figs. S18 and S19) and in water-in-salt electrolytes (fig. S18), where little water is available (*24*).

Further evidence for increasing effective ion size with increasing scan rate was obtained from electrochemical quartz crystal microbalance measurements of the scan rate dependence of weight increase per injected charge for a CNT sheet stack containing 40 wt % PSS. The transported water increased monotonically with increasing potential scan rate from 10 to 100 mV/s for the PSS@CNT sheet stack, whereas it was approximately constant for a neat CNT sheet stack (fig. S8). These weight change measurements during CV scans (fig. S7) also show unipolar weight pickup for the 40 wt % PSS@CNT sheet stack and bipolar weight pickup for the neat CNT sheet stack.

The effect of SRES can also be seen for actuation of a 30 wt % PSS@CNT yarn in 0.1 M aqueous LiCl electrolyte when using the large square-wave potentials enabled by unipolar behavior (Fig. 2C). The small stroke observed for a neat CNT yarn rapidly decreased with frequency increase because of capacitance decrease. The existence of SRES means that an increase in effective ion size partially compensates for this capacitance decrease. The maximum contractile work capacity for the unipolar PSS@CNT muscle is 0.73 J/g (Fig. 2D), which is 3.1 times that reported (*4*) for a CNT yarn operated in an aqueous electrolyte. These PSS@CNT unipolar muscles provided 10,000 largely reversible cycles (fig. S13) and a natural latching state (fig. S14). This SRES-enhanced contractile work capacity can be further increased to 3.5 J/g in an organic electrolyte because of its larger electrochemical window (fig. S9).

Because of the high rate capability of the unipolar PSS@CNT muscles, they can function at lower temperatures than prior-art electrochemical muscles. More specifically, the results of figs. S15 and S16 show that a 35 wt % PSS@CNT muscle can usefully operate down to −30°C while providing a contractile stroke of ~2.5%.

Unipolar actuation and SRES also occur for Nafion@CNT (Fig. 3A and fig. S29). The contractile work capacity of the Nafion@CNT reached 1.04 J/g (Fig. 3B), and the contractile efficiency (Fig. 3B) was 6.1% for a scan rate of 200 mV/s. An anion-exchange ionomer [poly (diallyldimethylammonium chloride), PDDA] shifts the pzc in an opposite direction (to below −1 V; fig. S5) to cation-exchange ionomers, but unipolar strokes and SRES are still obtained. A potential change from +1 to −1 V generates a −4.5% stroke for PDDA@CNT and a 5.8% stroke for PSS@CNT (fig. S30 and Fig. 2D). Unless the polymer in a CNT yarn contains a charged group, the pzc is little changed and no unipolar or SRES behavior is observed (fig. S21).

The capacitance (per CNT weight) of the PSS@CNT muscle substantially increases with increasing PSS content, which increases muscle stroke (figs. S6 and S32). Also, the concentration dependence of capacitance of the fully coiled PSS@CNT muscle is close to that for the precursor PSS@CNT sheet stack. The most reasonable explanation for this is that infiltration of PSS between nanotube bundles interferes with capacitance losses because of electrolyte wetting–induced and twist-induced increases in bundling.

Because PSS@CNT and PDDA@CNT yarns actuate in-phase when used as opposite electrodes, they can be mechanically coupled to provide a single muscle that uses the SRES-enhanced strokes of both yarns to increase the force output and eliminate the need for a passive counter electrode. An all-solid-state PSS@CNT/PDDA@CNT muscle coupled with gel electrolyte was realized (figs. S1 and S30), the contractile stroke of which (3.9%) was comparable to that for a PSS@CNT muscle (5.8%) and a PDDA@CNT muscle (4.5%). This elimination of an electrolyte bath is important for many applications. We used these coiled PSS@CNT and PDDA@CNT muscles to make an actuating two-layer textile (fig. S31), which shows a 3.9% contractile stroke in the warp direction

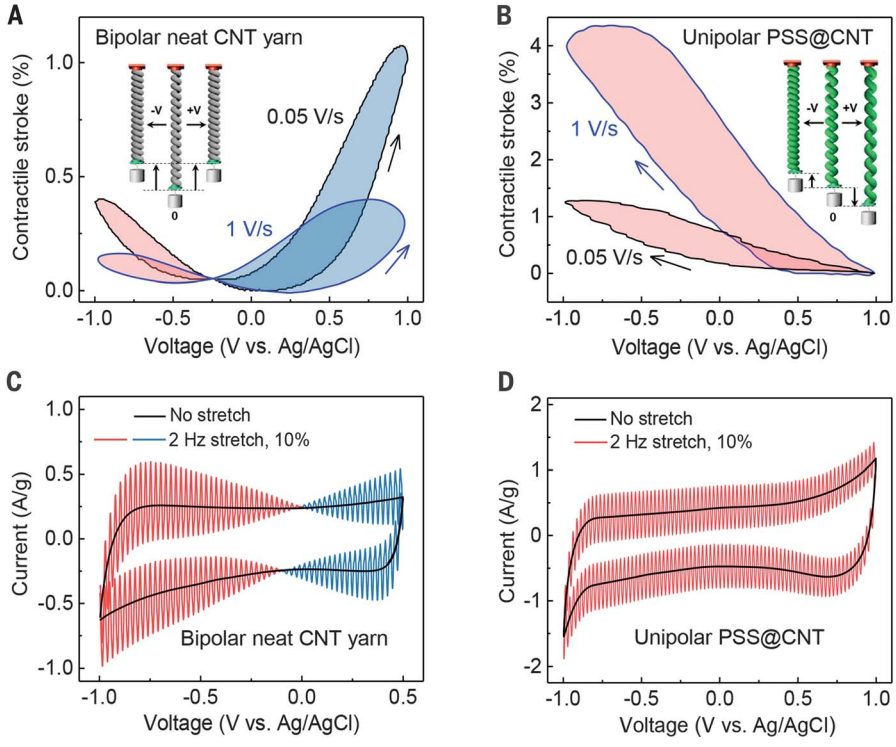

Fig. 1. Comparisons of unipolar and bipolar muscles. (**A** and **B**) Tensile stroke measurements under 10.9 MPa stress for different cyclic voltammetry scan rates for a neat CNT yarn muscle and a 30 wt % PSS@CNT yarn muscle, respectively, in 0.1 M aqueous LiCl. Insets are illustrations of bipolar and unipolar stroke actuation. (**C** and **D**) Piezoelectrochemical spectroscopy for a scan rate of 50 mV/s for a neat CNT yarn muscle and a 30 wt % PSS@CNT yarn muscle, respectively, in the above electrolyte. A sinusoidal tensile strain of 10% at 2 Hz was applied. The potential at which the stretch-induced current change vanishes indicates that the pzc of the neat CNT yarn is −80 mV and that the pzc of the unipolar PSS@CNT yarn is outside the electrochemical window of the electrolyte.

(the muscle direction) for a 0.05-Hz square wave between −2 and +2 V (movie S1).

A unipolar stroke, SRES, and 8000 largely reversible cycles were observed for a coiled CNT yarn muscle coated with a surfactant, sodium dodecyl sulfate (SDS) (figs. S22 and S24). The work capacity for square-wave excitation reached 0.79 J/g, and the maximum average power density during contraction and the full cycle power density were 2.7 and 2.0 W/g, respectively (Fig. 3C). Using this approach for a sheath-run artificial muscle (*19*), we obtained a usable muscle stroke (1.3%) when operating at 10 Hz in a 0.2 M LiCl aqueous electrolyte containing 0.6 wt % SDS (fig. S25B). This high frequency capability results from the combination of SRES behavior and the short diffusion distance for actuating the sheath compared with the diffusion distance for actuating a CNT yarn that has the same mass of CNTs per muscle length. Results for an aqueous LiCl electrolyte (Fig. 3D) show that the SCR is similarly enhanced with increasing potential scan rate for PSS@CNT and SDS@CNT muscles.

We also made unipolar muscles that provided 10,000 largely reversible cycles by biscrolling graphene oxide (GO) into a CNT yarn (figs. S26 and S27). During biscrolling, a GO-coated CNT sheet stack is twisted so that this guest is trapped within the helical corridors of the yarn (*25*). An organic electrolyte (0.2 M TBA·PF_6 in acetonitrile, where TBA is tetrabutylammonium) was used. With increasing GO content, the stroke of a CNT yarn muscle gradually changed from bipolar to unipolar (fig. S27). The peak equilibrium tensile contraction and work capacity were 21% and 4.1 J/g, respectively, compared with 16% and 3.2 J/g for the neat yarn in this electrolyte (Fig. 3E).

The contractile stroke of a unipolar GO@CNT muscle at 1 Hz was 8.0% (Fig. 3F) compared with 2.5% for the neat CNT muscle and the previous 4.7% for a sheath-run CNT muscle (*18*) at 1 Hz. The full-cycle contractile power and the maximum average power during contraction were 2.08 and 8.17 W/g, respectively, for the GO@CNT muscle, compared with 1.02 and 2.52 W/g, respectively, for a neat CNT yarn muscle (Fig. 3F). The highest previously reported full-cycle contractile power and maximum contractile average power for operation in an organic electrolyte were 0.99 and 3.71 W/g, respectively, for a sheath-run artificial muscle (*18*). Oxidizing the surfaces of the CNTs in a yarn using boiling nitric acid also results in unipolar behavior (with the maximum stroke twice that of the neat bipolar CNT yarn), but SRES was absent (fig. S28). Additional examples of unipolar strokes without SRES are found for Faradaic muscles (*15*, *16*) and those based on CNTs (fig. S20).

Our density functional theory (DFT) calculations show that the work function shift of the positive groups [$N^+(CH_3)_2$] in PDDA and the negative groups (SO_3^-) in PSS are identical in magnitude for the same ratio of charge to electrochemically accessible surface carbon atoms. Using the previously predicted linear correlation between pzc and work function (*26*), good agreement was obtained between the measured and calculated dependence of pzc on surface charge density (fig. S35). We found that coiled muscles containing electronically contacting neat CNT- and PSS-infiltrated yarns have a measured pzc that is the average of the component structures (figs. S33 and S34).

The variation of current density with potential for constant scan-rate actuation partially explains why muscle strokes are additive for galvanostatic stroke changes for different potential ranges (figs. S12 and S23), but they are not additive for fast constant scan-rate actuation or for square-wave actuation (fig. S10). Also, the sum of the charge injected at high potential scan rates for a potential scan from V_1 to V_3 is larger than the sum for a potential scan from V_1 to V_2 and from V_2 to V_3, where $V_3 > V_2 > V_1$ (fig. S11). Likewise, for high-frequency square-wave actuation, the charge injected for a potential change between V_1 and V_3 is larger than the sum of the charge injected for potential changes between V_1 and V_2 and between V_2 and V_3. This aspect has not been previously described because previous electrochemical muscles had such a low tensile stroke for fast actuation that it could not be investigated.

Performance improvements resulted from using coiled CNT yarns containing pzc shift agents such as ionomers, oxidized graphene platelets, and surfactants. These include avoiding stroke cancelation caused by bipolar actuation, enabling operation down to at least −30°C, realizing large strokes at high frequencies, and increasing efficiencies, work capacities, and power densities. These result from replacement of bipolar behavior with unipolar behavior and a marked increase in effective ion size caused by electroosmotic solvent pumping. The advantages of these unipolar muscles having SRES are also demonstrated for all-solid-state muscles and muscle textiles that eliminate the need for an electrolyte bath.

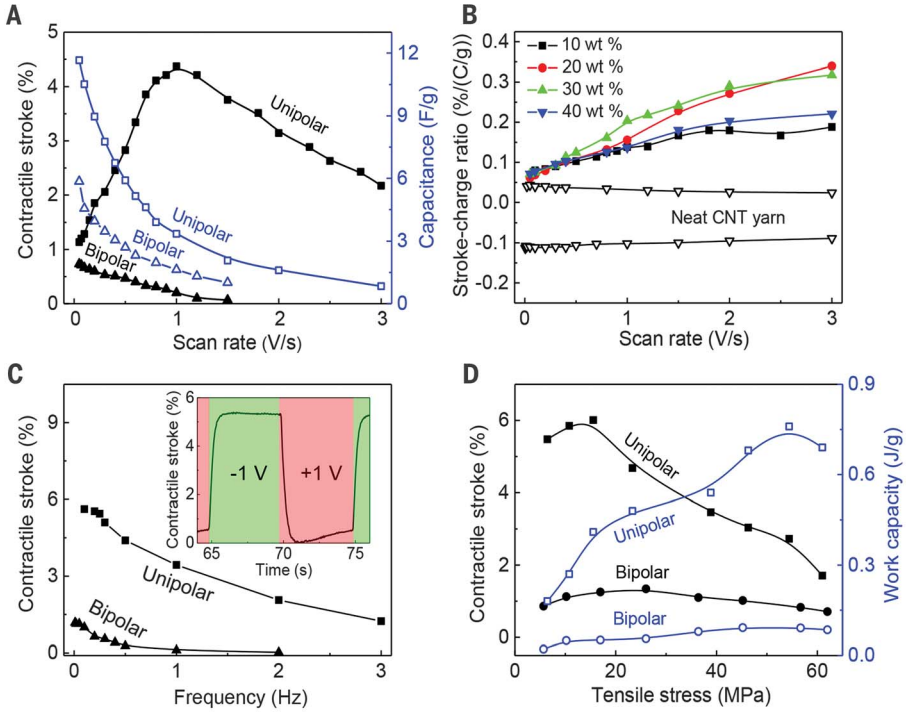

Fig. 2. Scan rate–enhanced strokes for PSS@CNT unipolar muscles. (**A**) Dependence of tensile stroke and capacitance on scan rate for a unipolar PSS@CNT and a bipolar neat CNT muscle in 0.1 M aqueous LiCl. Upon increasing the scan rate from 20 to 1000 mV/s, for the potential range of +1 to −1 V, the contraction of the unipolar muscle was amplified by a factor of 3.8. (**B**) Effect of polymer content on the stroke-charge ratio for a PSS@CNT unipolar muscle (for the potential range of −0.95 to 0.90 V) and for a bipolar CNT muscle (between −1.00 and 0.00 V and between 0.00 and 1.00 V). (**C**) Frequency dependence of contractile stroke for square-wave pulses, which is maximized by using a potential range between +1 V and −1 V for the above unipolar muscle and between 0 and +1 V for the bipolar muscle. The inset shows the dependence of stroke on square-wave pulses for the PSS@CNT muscle. (**D**) Dependence of equilibrium stroke and work capacity on applied tensile stress for a unipolar PSS@CNT muscle and a bipolar neat CNT muscle, when 0.1-Hz square-wave pulses are applied for the potential range in (C).

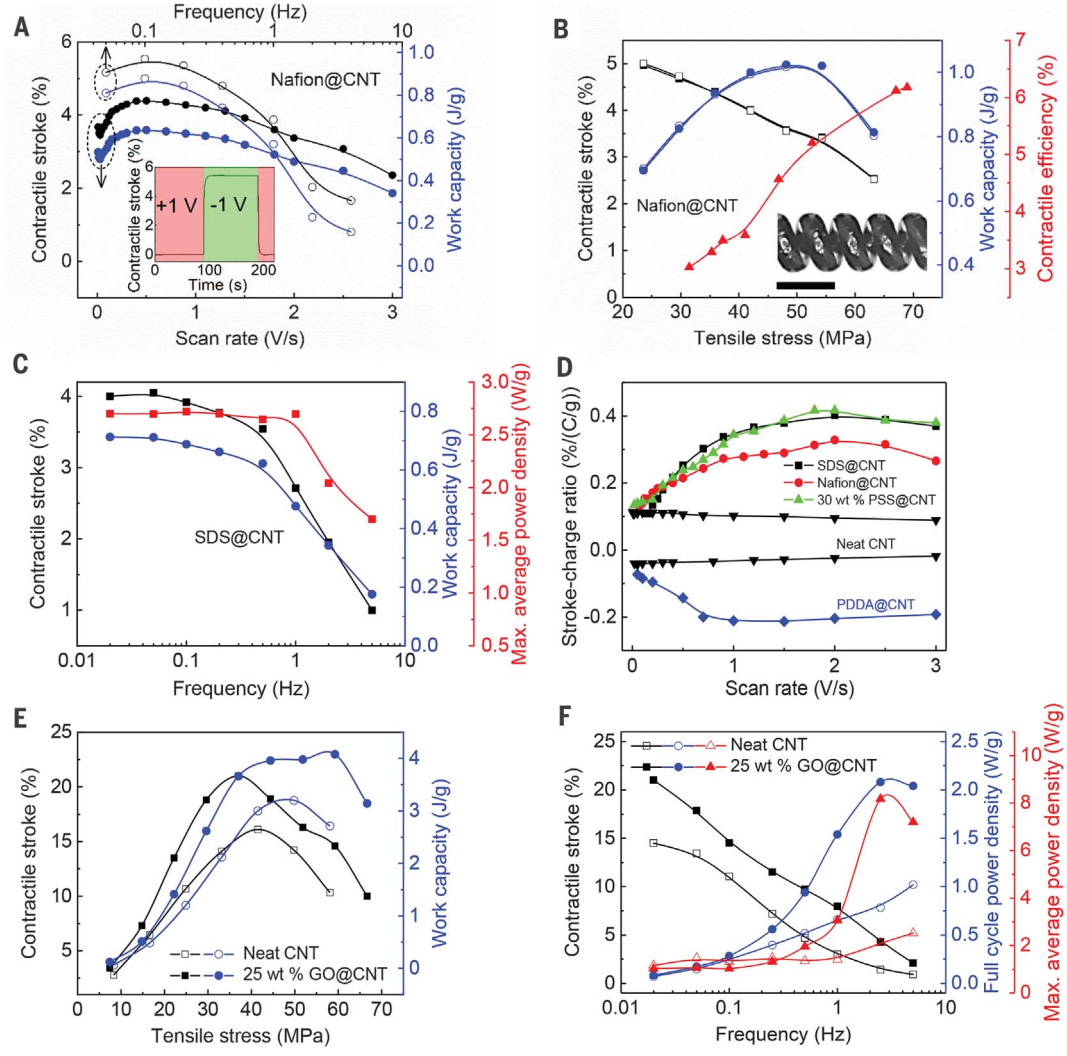

Fig. 3. Other unipolar muscles. (**A**) Dependence of muscle stroke and work capacity on scan rate (bottom axis) and on square-wave frequency (top axis) for a potential change between −1 and +1 V for a Nafion@CNT muscle operated in 0.2 M aqueous LiCl under 21 MPa tensile stress. The inset shows the dependence of stroke on square-wave pulses for the Nafion@CNT muscle. (**B**) Contractile stroke, work capacity, and contractile efficiency versus tensile stress for the Nafion@CNT muscle, when 0.1-Hz square-wave pulses are applied for the potential range and electrolyte in (A). The inset shows a microscope image of the Nafion@CNT muscle. Scale bar, 150 μm. (**C**) Dependence of contractile stroke, work density, and maximum average power density on square-wave frequency for an SDS@CNT muscle having 48 MPa applied load. (**D**) Stroke-charge ratio versus potential scan rate for unipolar muscles having SRES and a bipolar neat CNT muscle that does not have SRES. The electrolyte used was 0.1 M LiCl for PSS@CNT, PDDA@CNT, and the neat CNT yarn and 0.2 M LiCl for Nafion@CNT and SDS@CNT. (**E**) Contractile stroke and work capacity versus applied tensile stress for neat CNT yarn and 25 wt % GO@CNT yarn when actuated in 0.2 M TBA·PF_6 in acetonitrile at a square-wave frequency of 0.02 Hz and a potential change from −2.75 to +1 V. (**F**) Contractile stroke, full-cycle power density, and maximum average power density versus square-wave frequency for actuation of a neat CNT yarn and a 25 wt % GO@CNT yarn using the above electrolyte and potential range and 36 MPa applied load.

REFERENCES AND NOTES

1. S. M. Mirvakili, I. W. Hunter, *Adv. Mater.* **30**, 1704407 (2018).
2. J. D. Madden, *Science* **318**, 1094–1097 (2007).
3. G.-Z. Yang *et al.*, *Sci. Robot.* **3**, eaar7650 (2018).
4. R. H. Baughman *et al.*, *Science* **284**, 1340–1344 (1999).
5. Y. Yun *et al.*, *Nano Lett.* **6**, 689–693 (2006).
6. J. Foroughi *et al.*, *Science* **334**, 494–497 (2011).
7. J. Qiao *et al.*, *Small* **14**, e1801883 (2018).
8. J. A. Lee *et al.*, *Adv. Mater.* **29**, 1700870 (2017).
9. K. J. Kim *et al.*, *ACS Appl. Mater. Interfaces* **11**, 13533–13537 (2019).
10. C. S. Haines *et al.*, *Science* **343**, 868–872 (2014).
11. J. Fan, G. Li, *RSC Advances* **7**, 1127–1136 (2017).
12. M. Kanik *et al.*, *Science* **365**, 145–150 (2019).
13. M. Hiraoka *et al.*, *Sci. Rep.* **6**, 36358 (2016).
14. P. Chen *et al.*, *Nat. Nanotechnol.* **10**, 1077–1083 (2015).
15. W. Lu, E. Smela, P. Adams, G. Zuccarello, B. R. Mattes, *Chem. Mater.* **16**, 1615–1621 (2004).
16. K. Mukai, K. Yamato, K. Asaka, K. Hata, H. Oike, *Sens. Actuators B Chem.* **161**, 1010–1017 (2012).
17. A. González, E. Goikolea, J. A. Barrena, R. Mysyk, *Renew. Sustain. Energy Rev.* **58**, 1189–1206 (2016).
18. Materials and methods are available as supplementary materials.
19. J. Mu *et al.*, *Science* **365**, 150–155 (2019).
20. S. H. Kim *et al.*, *Science* **357**, 773–778 (2017).
21. T. Okada, H. Satou, M. Okuno, M. Yuasa, *J. Phys. Chem. B* **106**, 1267–1273 (2002).
22. M. D. Bennett, D. J. Leo, G. L. Wilkes, F. L. Beyer, T. W. Pechar, *Polymer (Guildf.)* **47**, 6782–6796 (2006).
23. S. Nemat-Nasser, Y. Wu, *J. Appl. Phys.* **93**, 5255–5267 (2003).
24. L. Suo *et al.*, *Science* **350**, 938–943 (2015).
25. M. D. Lima *et al.*, *Science* **331**, 51–55 (2011).
26. S. Trasatti, *J. Electroanal. Chem. Interfacial Electrochem.* **33**, 351–378 (1971).

ACKNOWLEDGMENTS

We thank B. J. Carlson, H. L. Hansen, and X. Li for sample preparation and measurements. **Funding:** Support in the United States was from Air Force Office of Scientific Research grant no. FA9550-18-1-0510, Robert A. Welch Foundation grant no. AT-0029, and DARPA SHRIMP program contract no. HR001119C0042. Support in Korea was from the Creative Research Initiative Center for Self-Powered Actuation of the National Research Foundation of Korea and the Ministry of Science and ICT and the National Research Foundation of Korea (grant nos. 2012R1A3A2048841 and 2015M3D1A1068062). Support in China was from the Program of Introducing Talents of Discipline to Universities (grant no. G20212006001), the National Key Research and Development Program (grant no. 2017YFB0307001), the National Natural Science Foundation (grant no. 91648109), the Harbin Institute of Technology program for short-term PhD visits, and the China Scholarships Council. Support in Australia was from the Alfred Deakin Postdoctoral Research Fellowship and the Australian Research Council (grant no. FT130100380). **Author contributions:** R.H.B. conceived and initiated the project. All authors contributed to experimental design, planning, and execution; data analysis; and manuscript writing. H.K., P.C., M.C., K.C., S.N., and K.A.A. conducted theoretical analysis. **Competing interests:** H.C., J.L., X.H., N.L., C.S.H., S.F., Z.W., J.M., and R.H.B. are listed as the inventors on a PCT patent application (PCT/US2020/016391) describing unipolar muscle. **Data and materials availability:** All data needed to evaluate the conclusions in the study are present in the main text or the supplementary materials.

SUPPLEMENTARY MATERIALS

science.sciencemag.org/content/371/6528/494/suppl/DC1
Materials and Methods
Supplementary Text
Figs. S1 to S35
Caption for Movie S1
References (*27*–*39*)
Movie S1

24 April 2020; accepted 17 December 2020
10.1126/science.abc4538

Unipolar stroke, electroosmotic pump carbon nanotube yarn muscles

Hetao Chu, Xinghao Hu, Zhong Wang, Jiuke Mu, Na Li, Xiaoshuang Zhou, Shaoli Fang, Carter S. Haines, Jong Woo Park, Si Qin, Ningyi Yuan, Jiang Xu, Sameh Tawfick, Hyungjun Kim, Patrick Conlin, Maenghyo Cho, Kyeongjae Cho, Jiyoung Oh, Steven Nielsen, Kevin A. Alberto, Joselito M. Razal, Javad Foroughi, Geoffrey M. Spinks, Seon Jeong Kim, Jianning Ding, Jinsong Leng and Ray H. Baughman

Science **371** (6528), 494-498.
DOI: 10.1126/science.abc4538

Pump it up

Carbon nanotube yarns can be used as electrochemical actuators because infiltration with ions causes a contraction in length and an expansion in diameter. Either positive or negative ions can cause this effect. Chu *et al.* constructed an all-solid-state muscle that eliminated the need for an electrolyte bath, which may expand the potential for its use in applications. By infiltrating the yarns with charged polymers, the fibers start partially swollen, so the length can increase through the loss of ions. It is thus possible to increase the overall stroke of the muscle. Further, these composite materials show a surprising increase in stroke with scan rate.

Science, this issue p. 494